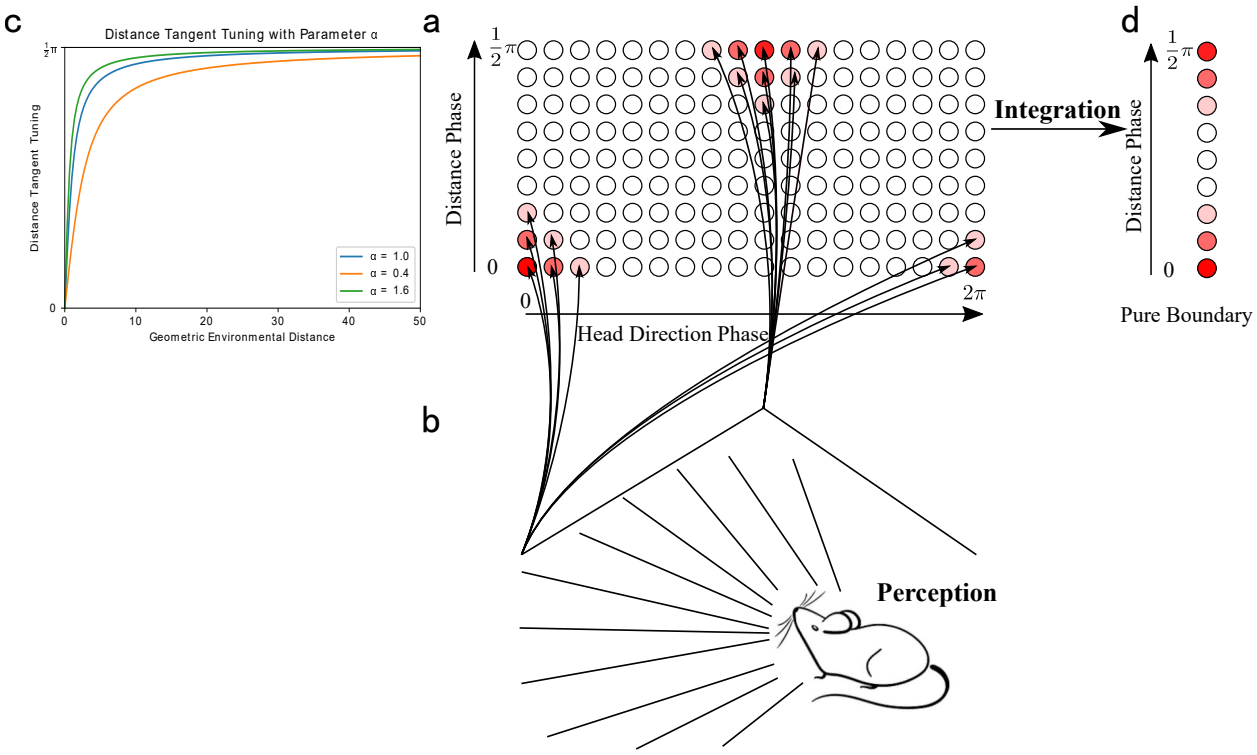

Figure S 1. Neural population of boundary representations. (**a**) Model neurons encoding the conjunction of boundary distance and bearing form a two-dimensional neural manifold. (**b**) The perceived distance of the boundaries in the environment is mapped nonlinearly to the distance dimension of the neural manifold, and the boundary orientation is mapped linearly to the direction dimension of the manifold. Depending on the input, an activity pattern emerges in the network and encodes the geometry of the local space defined by the perceived boundaries. (**c**) The nonlinear mapping of the boundary distance to the distance dimension of the manifold. Parameter α controls the steepness of the mapping. (**d**) The conjunctive encoding of the distance and orientation of the boundary can be integrated along the direction dimension by another group of units to encode the distance of the boundary.

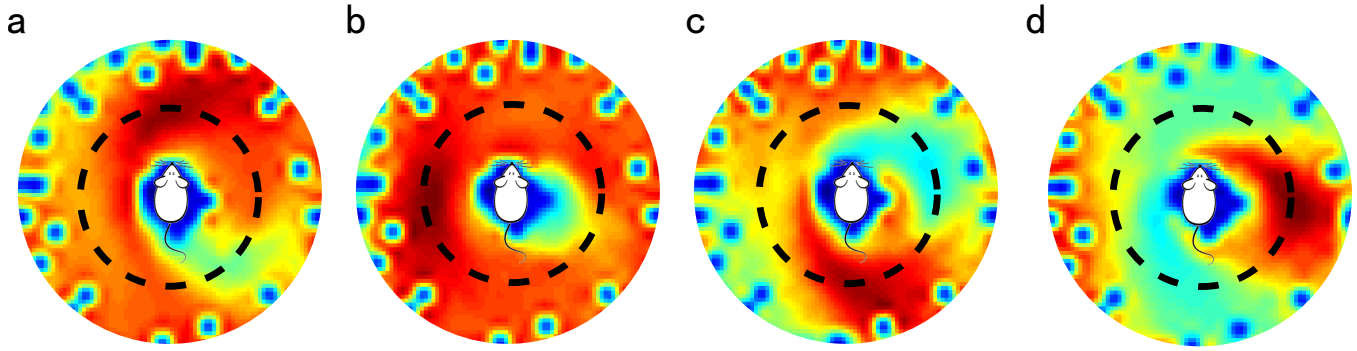

Figure S 2. Firing rate maps of egocentric boundary units in the egocentric reference frame (Eq. 2). The rat is located in the center of the firing map, and the activity of the firing map represents the activity of one example unit in response to the wall relative to the rat at a given egocentric direction and distance. The black ring shows the distance from the rat with the maximal firing rate. (**a**), (**b**), (**c**), and (**d**) show the firing rate maps of four different egocentric boundary units with preferred bearings (0, $\frac{1}{2}\pi$, π, $\frac{3}{2}\pi$), respectively. Zero degrees corresponds to the front of the animal. The same jet colormap is used to code firing rates increasing from zero to the maximum using blue to red.

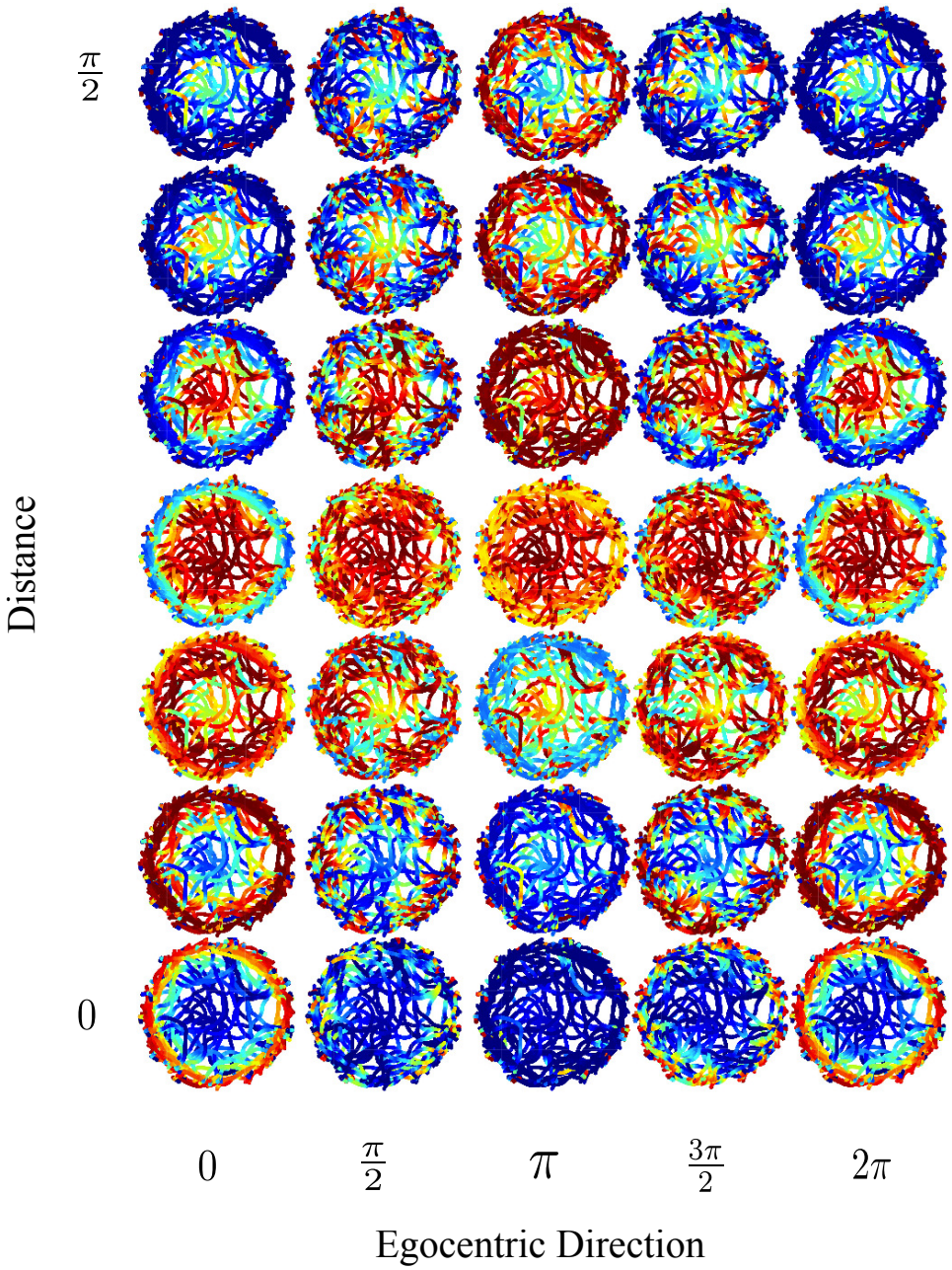

Figure S 3. Firing rate maps of egocentric boundary units in the allocentric reference frame (Eq. 2). The firing rate maps of 28 example egocentric boundary units are arranged from left to right for increasing preferred boundary bearings and from bottom to top for increasing preferred boundary distances. The fifth column is the same as the first column due to the periodicity of angles. The same jet colormap is used to code firing rates increasing from zero to the maximum using blue to red.

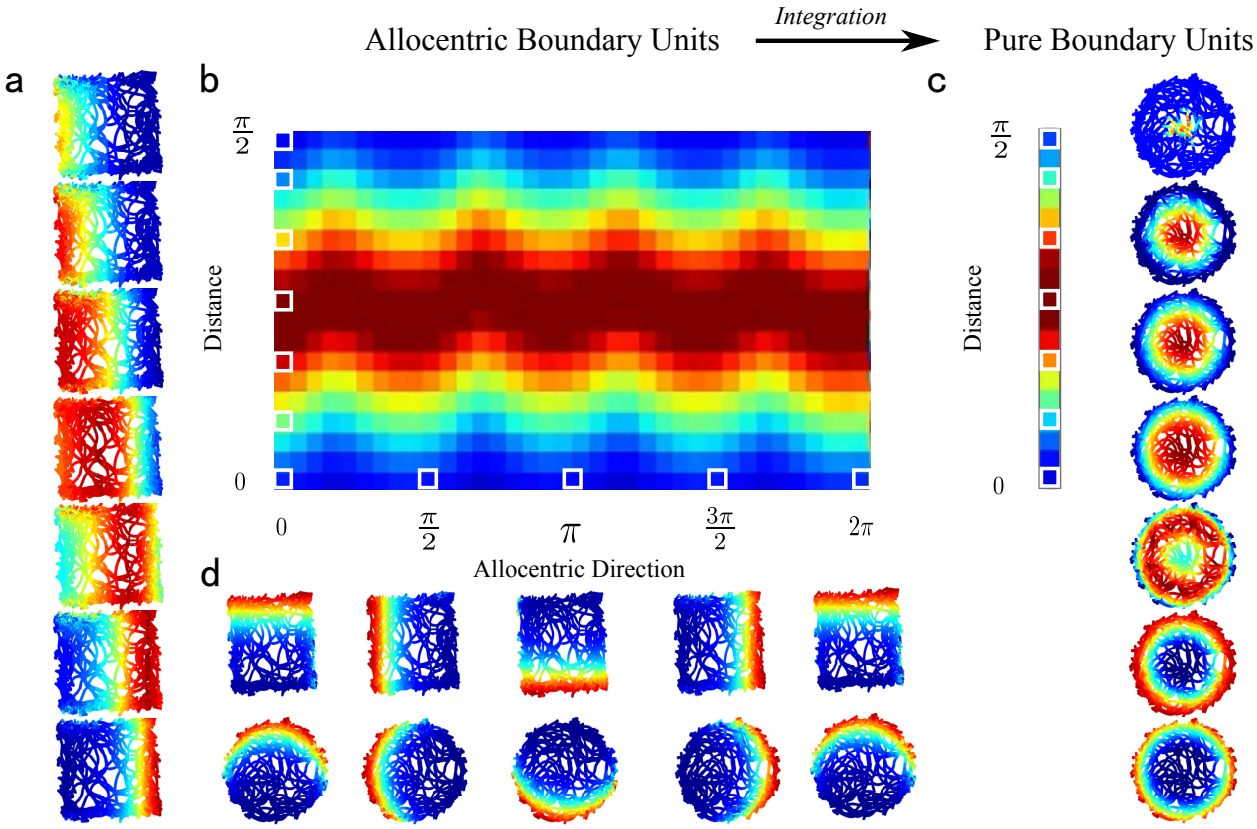

Figure S 4. Boundary representation in the allocentric reference frame. (**a**) Firing rate maps within a square maze of allocentric boundary units marked in white boxes in the left column of (**b**). (**b**) One example of the population activities of allocentric boundary units within a box maze. (**c**) Pure boundary units integrate the activity of allocentric boundary units. Depending on the preferred distance, pure boundary units show spatial firing patterns in a cylinder maze, resembling those of bulls-eye cells, annulus cells, and circular-ring cells. Firing maps are shown for the units marked by white boxes. (**d**) Allocentric border units that prefer proximal boundaries express firing fields at the borders in walled square and circle environments. Firing maps correspond to the units marked in white boxed in the bottom row of (**b**). (**a**), (**b**), and (**d**) are formed by allocentric boundary cell model (Eq. 3); (**c**) by pure boundary cell model (Eq. 4).

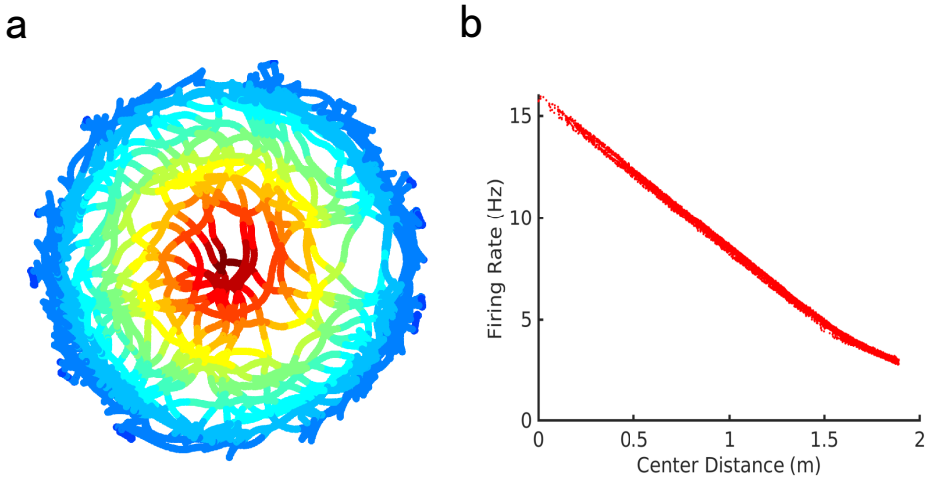

Figure S 5. The firing rate maps of a center-distance unit with negative distance tuning (obtained after the integration of Eq. 8). (**a**) The unit shows a decreased firing rate trend away from the geometric center (left). (**b**) The firing rate negatively correlates with center-distance.

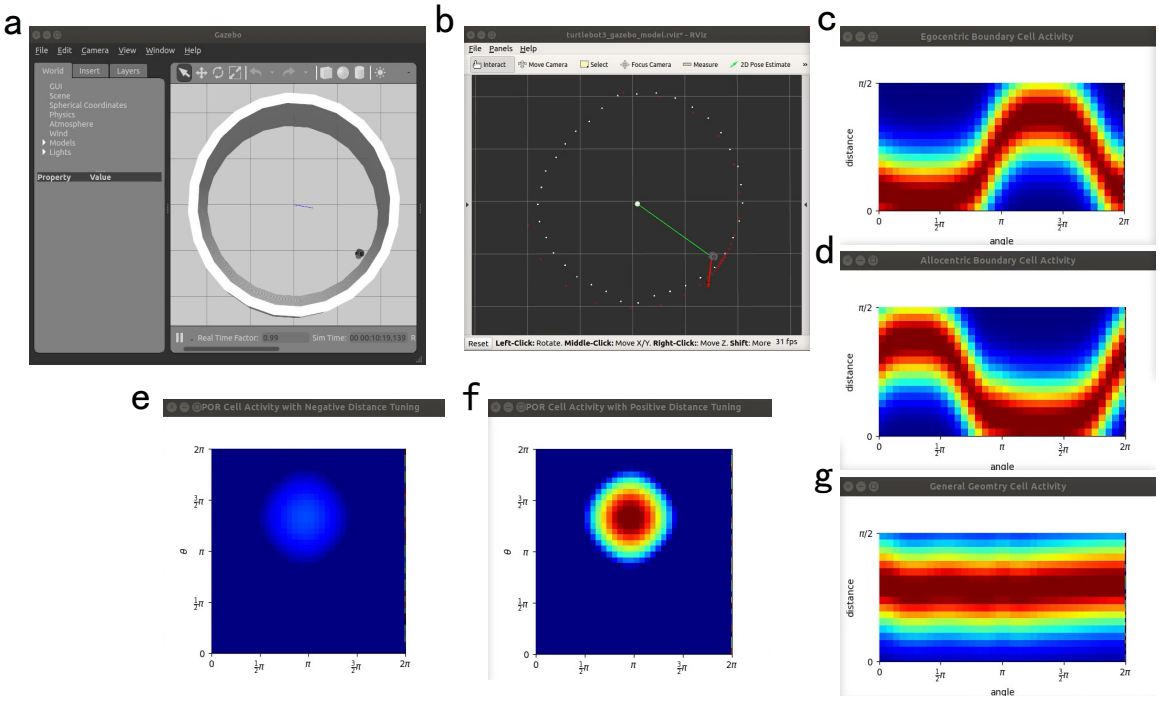

Figure S 6. Screenshots of the simulation of neural implementations. The neural activities are all rendered as heat maps. (**a**) The Gazebo simulation Environment; (**b**) The rviz for 3D visualizer; The neural activity of egocentric (**c**, Eq. 2) and allocentric (**d**, Eq. 3) boundary units; The neural activity of conjunctive center-bearing units with negative (**e**) and positive (**f**) distance tuning (Eq. 8); (**g**) The neural activity of geometry units (Eq. 9).

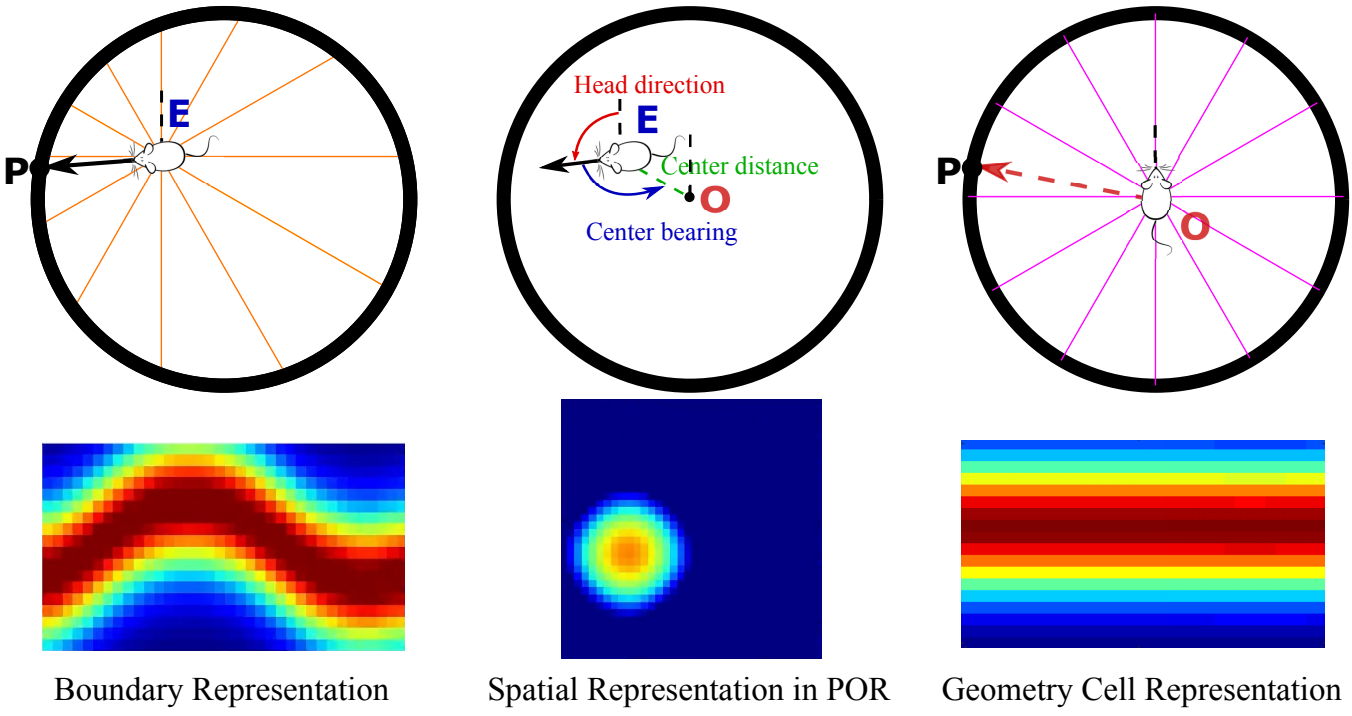

Figure S 7. The formation of the geometry cell representation. The geometry representation and the spatial representation in POR emerge from the egocentric spatial representation of environmental boundaries. The conjunctive center bearing cell model conjunctively encodes the egocentric bearing and the animal's allocentric head direction, as well as the distance of the geometric center. The geometry cell model forms a topographic representation of spatial layouts of the local scenes in disparate environments, as a possible foundation for high-level efficient topographic cognitive maps.

Movie 1. The robot randomly explores in a cylinder maze. Refer to Figure S6 for the specific description of each window in the movie.
Movie 2. The robot randomly explores in a square maze.
Movie 3. The robot randomly explores in a pentagon maze.
Movie 4. The robot randomly explores in a concave environment with two convex mazes connected by a narrow corridor.
Movie 5. The robot explores in a virtual office environment manually teleoperated through a keyboard. The topological cognitive map and the occupancy grid map are simultaneously constructed for comparison. The colored area is the local space of the environment encoded by a geometry representation. The boundaries vectors are color-coded by the distance along the x-axis. The green dots and red lines are the vertices and edges of the cognitive map, respectively. Each vertex in the cognitive map is associated with a geometry representation. The blue line is the running trajectories of the robot.